Conformations and Rotational Barriers of Aromatic Polyesters

P. Lautenschläger and J. Brickmann

Technische Hochschule Darmstadt, Institut für Physikalische Chemie I, Petersenstrasse 20, 6100 Darmstadt, Germany

Jippe van Ruiten and Robert J. Meier*

DSM Research, P.O. Box 18, 6160 MD Geleen, The Netherlands

Received July 10, 1990

ABSTRACT: An integrated approach employing ab initio, semiempirical (AM1), and force field (CVFF) methods to study torsional barriers in conjugated aromatic molecular systems is presented. It is the *first* time that such an attempt including *full* geometry optimization up to the ab initio level is reported. We have focused on monomer-like units of poly(*p*-hydroxybenzoic acid) (PHBA) and poly(ethylene terephthalate) (PET). Coupling between the torsional motions was studied with the semiempirical AM1 method as well as with the consistent valence force field. Molecular dynamics simulations were carried out on single chains; the relation between MD results and chain flexibility is discussed as well as the consequences of the uncertainty in barrier heights for the MD results and the calculated persistence length. The numerical results are compared with experimental data as far as such data are available. Large differences between various theoretical results are observed, indicating that there are problems with the modeling of rotational barriers in aromatic moieties containing substituents which are π-conjugated to the aromatic ring. This as well as the lack of sufficient and accurate experimental data hampers progress in modeling the properties of the conjugated aromatic molecules investigated here.

1. Introduction

The past few years have seen a strongly growing interest in the theoretical modeling of synthetic polymers because of recent developments with regard to both theoretical techniques and computer resources. A thorough understanding of properties and processes at the molecular level could increase our knowledge to such an extent that it is legitimate to expect, on a midterm time scale, the guided development of new chemicals and polymers.

One important characteristic of a polymer chain is its *conformation*, as it is directly related to the structure of both the crystalline and amorphous states, thus determining mechanical properties, optical properties (nonlinear optical materials), electrically conducting properties, and the stiffness of polymer chains (liquid crystalline polymers (LCP's)). The single-chain conformation is mainly determined by the rotational degrees of freedom. A theoretical approach therefore involves the determination of the corresponding rotational barrier heights. The accuracy of the calculated energies is highly dependent on the parametrization of the force fields and the approximations and parametrization of the semiempirical methods, respectively, whereas for the ab initio calculations the size of the basis set is an important factor. The purpose of this paper is essentially to discuss the merits of these three methods in relation to torsional barriers in aromatic moieties, e.g., terephthalic acid and monomers of poly(*p*-hydroxybenzoic acid) (PHBA) and poly(ethylene terephthalate) (PET). These monomers or their derivatives are common entities in LCP's and are also of relevance as model compounds for lubricants (e.g., (2-ethylhexyl)benzoic acid) and are excellent plasticizers in PVC (alkyl phthalates).

In principle, the full potential energy function can be calculated with the aid of all three theoretical methods mentioned above, though it turns out to be difficult to find full calculated torsional energy profiles in the literature; profiles have only been calculated for small systems such as ethane and dimethoxymethane,[1] but lack even for a system such as propanal.[2] Schaefer and Penner[3] were the only ones to report ab initio potential energy curves including geometry optimization for the class of systems we are interested in, phenyl derivatives, whereas more recently the first semiempirical results have been published.[4]

To test the reliability of a method it is necessary to compare calculated data with experimental data. Unfortunately, relevant experimental data are only available for small molecules. For phenol,[5] benzaldehyde,[6] and benzoyl fluoride[7] the barrier height was inferred from microwave gas-phase data, whereas experimental data on other small aromatic molecules were obtained from far-infrared spectra of both gases and liquids.[8] Information on larger systems should be unveiled from solid-state data by analyzing vibrational spectra[9] or by studying mechanical and dielectric relaxation phenomena.[10,11] The latter method unfortunately involves tedious work in assigning observed loss peaks to particular molecular rotations and in polymers usually yields but a single barrier height. Analyzing vibrational spectra requires assignment of all relevant vibrational frequencies and usually examination of deuterated species. It was noted by Miller et al.[8] that, due to intramolecular interactions, torsional barriers obtained from liquid-state infrared data can be up to twice as high as those from gas-phase infrared spectra. As a consequence one should exercise extreme care when comparing calculated and experimental torsional barrier heights other than those referring to gas-phase data.

None of the experimental techniques will give us definitive information on the exact *form* of the potential energy curve between the minimum energy and the barrier for the systems considered here. We therefore adopt the following working hypothesis: *the theoretical method that yields the best quantitative agreement with available experimental barrier heights is assumed to yield the best potential energy curve for intramolecular rotations.*

Let us now briefly outline the contents of the relevant papers in this field. One of the earlier relevant theoretical studies by ab initio techniques is that of Hehre et al.[12] reporting ab initio calculations at the STO-3G level of the conformations of monosubstituted benzenes. Only a few

0024-9297/91/2224-1284$02.50/0

particular conformations (minimum-energy structure and barrier height) were studied without full geometry optimization.

Hummel and Flory[13] used bond lengths and angles from experimental X-ray data in force field calculations on *p*-phenylene polyamides and polyesters. Employing an expression of the form $E_{deloc} = -B_\Phi \cos^2 \Phi$ for describing the contribution of π-electron delocalization to the rotational energy profiles, the latter were plotted for a range of B values. The B value finally adopted was that which fitted the X-ray data best. Coulombic terms were neglected. In an accompanying paper[14] these authors calculated a persistence length from a Boltzmann distribution of the accessible rotational states. However, the authors fixed a number of torsional angles, which casts serious doubt on the validity of their numerical data concerning persistence lengths and other properties, as was also noted by Jung and Schurmann.[15]

Schaefer et al.[16] computed structures and internal rotational barriers of phenol and a number of benzoyl derivatives. The ring was not fully optimized but nevertheless the overall structures and rotational barriers turned out to be in reasonable quantitative agreement as far as reliable experimental data were available. In a later paper Schaefer and Penner[3] reported full geometry optimizations at the STO-3G level for phenyl formate. The rotational energy profile of the phenyl formate torsion was calculated in 15° intervals in torsional angle. These results are particularly relevant with respect to PHBA, one of the systems that we have studied and that will be discussed here.

Konschin[9] analyzed low-frequency Raman spectra of some hydroxy- and methoxy-substituted benzenes in conjunction with ab initio calculations at the STO-3G level. Several schemes were tested such as standard geometries and both partial and full geometry optimization. Experimental data were largely from the solid state, and it turned out that several barriers were apparently strongly influenced by their environment.

Fabian[17] calculated conformations and rotational barriers of numerous conjugated molecules. From a comparison of ab initio results with available experimental data he concluded that rotational barriers calculated by the AM1 method were about 50% low. This conclusion was based on a few available experimental data only.

Coulter and Windle[4] carried out MNDO and AM1 calculations and parameterized aromatic esters for use in the MM2 force field program. This parametrization was carried out with what they call an "iterative intuitive fitting process" based on experimental data obtained by scanning the Cambridge Crystallographic Data Bank for all structures containing the phenyl benzoate moiety, which implies averaging of intermolecular interactions. As the intermolecular interaction energies are of the same order of magnitude as some barrier heights, a possibly large dense-state effect on the configuration and thus on the derived force field parameters is to be expected. A famous example is the conformation of biphenyl.[18] Another example is that of (2-ethylhexyl)benzoic acid, which exhibits a broadening and a shift of the infrared bands with increasing concentration.[19] These dense-state effects prevent a comparison and cross-check with vacuum-state semiempirical and ab initio calculations and comparison with the most accurate experimental data obtained from microwave gas-phase experiments (see previous reference to Miller et al.[8]). Secondly, the presence of strong coupling between rotations (concerted motion) makes it more likely that the fitted force field parameter set is just one out of many

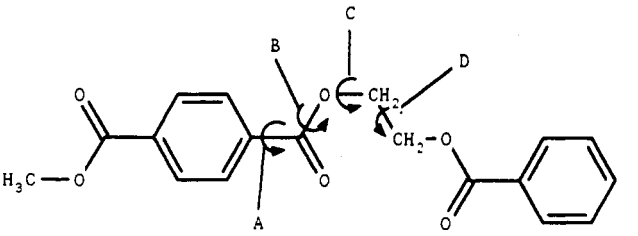

Figure 1. Model system for PET showing the torsional angles around the C_{phenyl}–$C_{carbonyl}$ (torsion A), the $C_{carbonyl}$–O_{ether} (torsion B), the $C_{aliphatic}$–O_{ether} (torsion C), and the $C_{aliphatic}$–$C_{aliphatic}$ (torsion D) bonds.

that yield the correct equilibrium conformations in the solid state (minimum energy) but does not necessarily work well for barrier heights and the form of the potential energy curve. Moreover, mixing of the intra- and intermolecular energy effects makes it less likely that structures different from those used during parametrization will be described well by the resulting force field, which is a bad starting point when using the method for predictive purposes in *molecular design*.

In some of the references[4,13,15] a force field is used that has not been sufficiently justified. Moreover, almost none of the calculations (except ref 3) are concerned with an analysis of the *form* of the potential energy curves related to the rotations, whereas in the case of a high barrier, the steepness of the well largely determines the accessible rotational states. It is for these reasons that we start from small (monomer-like) molecules and try to correlate experimental data with ab initio, semiempirical, and force field calculations. On the basis of this comparison we hope to arrive at an acceptable technique for modeling carboxylate-containing polymers.

The use of force field and semiempirical techniques allows the study of larger systems and consequently the study of coupling between rotations (concerted motion) and the effects of substituents. In order to test the reliability of such techniques and their calculated results, we have performed force field, semiempirical, and ab initio calculations using STO-3G and 3-21G basis sets on terephthalic acid; all calculations involved full geometry optimizations. Finally, we discuss results of some molecular dynamics (MD) simulations on PHBA and PET. At a later stage intermolecular interactions will be taken into consideration.

2. Computational Methods

Semiempirical calculations were carried out with the AM1 program[20] on an IBM 3090-VF of the computer center of the Technical University of Darmstadt. Ab initio calculations were carried out with the CADPAC program package[21] running on an IBM 3090 at the DSM Computing Centre CCN. Molecular mechanics calculations and molecular dynamics simulations were carried out with the INSIGHT/DISCOVER program package incorporating the consistent valence force field (CVFF)[22] and implemented on a Silicon Graphics 4D/70 GT workstation at DSM Research.

3. Results

We started off with AM1[20] calculations on the relevant torsional angles and energy profiles of the two model systems for PET (Figure 1) and PHBA (Figure 2). We will designate these compounds by their abbreviated polymer names PHBA and PET. Full geometry optimizations were carried out with 15° increments in torsional angles. In Figure 3 the resulting energy profiles including

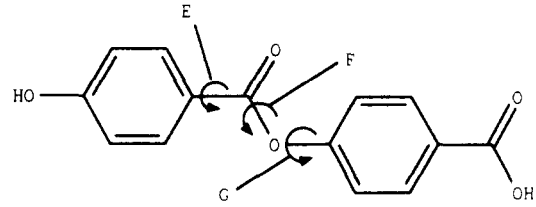

Figure 2. Model system for PHBA showing the torsional angles around the C_{phenyl}–$C_{carbonyl}$ (torsion E), the $C_{carbonyl}$–O_{ether} (torsion F), and the C_{phenyl}–O_{ether} (torsion G) bonds.

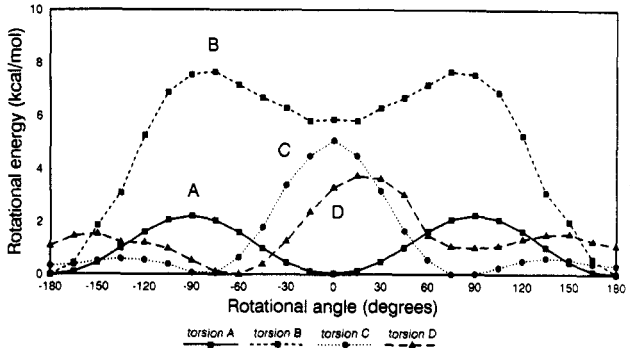

Figure 3. AM1-calculated rotational energy profiles for torsional angles A–D in PET. The marks on the curves indicate the data points that were calculated explicitly.

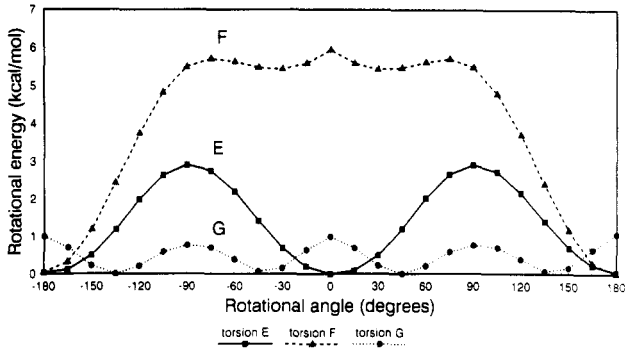

Figure 4. AM1-calculated rotational energy profiles for torsional angles E–G in PHBA. The marks on the curves indicate the data points that were calculated explicitly.

the barrier heights are depicted for the four rotations in PET. Figure 4 depicts the rotational energy profiles around the three torsional bonds in PHBA. We note here that in all figures we have not depicted smoothed curves through the data points in order to emphasize the originally calculated data points. The drawn lines are a guide to the eye.

The same molecules were studied with the CV force field. The results of full geometry optimizations are shown in Figures 5 and 6 for PET and PHBA, respectively.

In order to investigate the dependence of the rotational energy profile on the method of calculation more carefully and in view of the apparent differences between the CVFF and AM1 results, we have calculated the torsional barrier in terephthalic acid (Figure 7) with complete geometry optimization using ab initio (STO-3G and 3-21G basis sets), semiempirical (AM1), and force field (CVFF/DISCOVER) methods. Figure 8 shows all four calculated rotational energy profiles. In all calculations the torsional angle around the C_{phenyl}–$C_{carbonyl}$ bond was varied stepwise, whereas all other geometrical parameters were optimized.

MD simulations were carried out on a series of chains varying from flexible ones (polyethylene (PE)) to chains of intermediate stiffness (PET and PHBA) to stiff chains such as polyphenyl (pPh). The chains consisted of 30–50

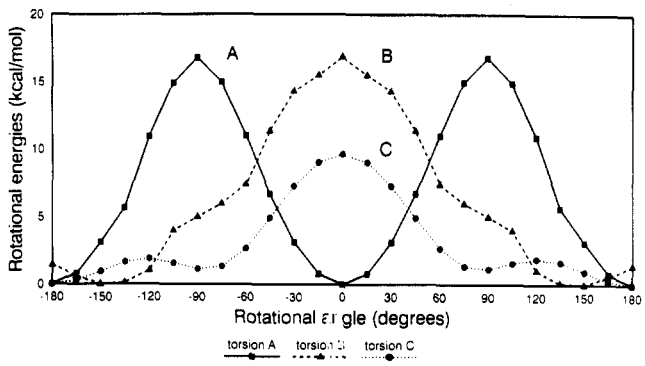

Figure 5. CVFF-calculated rotational energy profiles for torsional angles A–C in PET. The marks on the curves indicate the data points that were calculated explicitly.

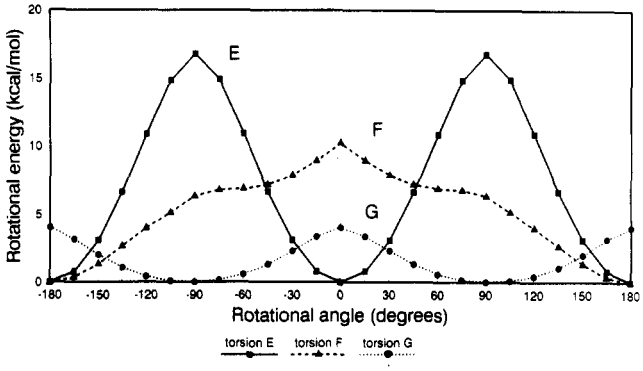

Figure 6. CVFF-calculated rotational energy profiles for torsional angles E–G in PHBA. The marks on the curves indicate the data points that were calculated explicitly.

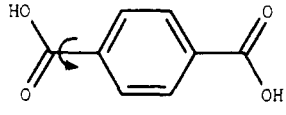

Figure 7. Terephthalic acid with torsional barrier as studied indicated.

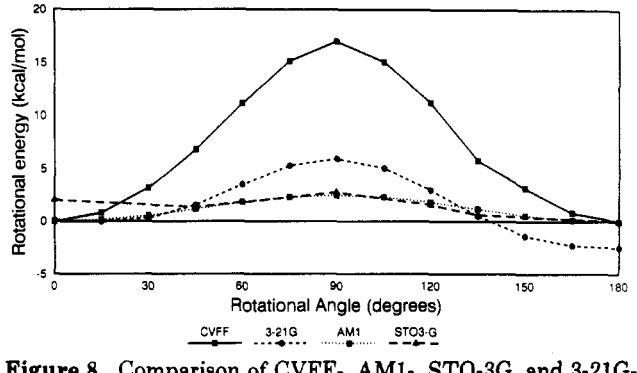

Figure 8. Comparison of CVFF-, AM1-, STO-3G, and 3-21G-calculated rotational energy profiles for the rotation of a carboxylic group in terephthalic acid as indicated in Figure 7. All data refer to fully optimized structures.

monomer units. The CVFF was employed without cross terms and without taking into account explicit charges. Hydrogen atoms were explicitly taken into account (i.e., no united-atom approach). Integration time during the MD simulation was 1 fs, whereas the simulations were carried out over several dozens of picoseconds. Figures 22–25 show snapshots of 10-ps intervals in the MD simulations of PE, PET, pHBA, and pPh.

4. Discussion

(a) AM1 Calculations. The AM1 results depicted in Figures 3 and 4 show that the torsional barriers in these

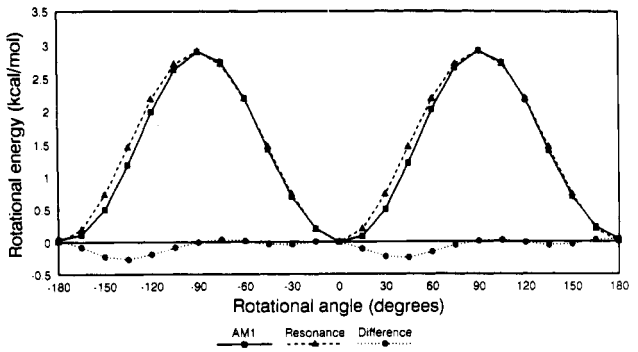

Figure 9. Torsional energy for torsion E of PHBA calculated by the AM1 method, the resonance stabilization energy reflected by a $\sin^2\theta$ dependence, and the remaining energy difference plot.

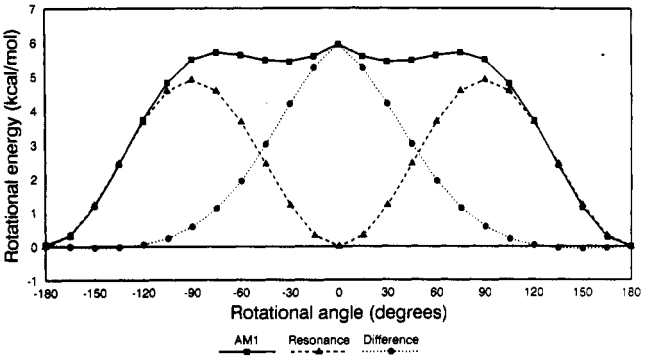

Figure 10. Torsional energy for torsion F of PHBA calculated by the AM1 method, the resonance stabilization energy reflected by a $\sin^2\theta$ dependence, and the remaining energy difference plot. The latter represents the steric interaction energy between a phenyl proton and the carbonyl oxygen.

two systems are between 0.5 and 8 kcal/mol. Since room temperature corresponds to about 0.6 kcal/mol, this implies that some barriers, typically up to say 3 kcal/mol (for comparison, the barrier in ethane amounts to 2.9 kcal/mol), are relatively insignificant in the sense that they will be overcome easily at room temperature. Higher barriers really contribute to the stiffness of the molecule. The energy profiles can be qualitatively understood assuming a resonance stabilization term (π-electron conjugation effect) and, if applicable, a steric hindrance term (van der Waals radii overlap). From the computations, largely on the basis of the calculations on terephthalic acid which are to be discussed later, it follows that the resonance effect is to be described by a $\sin^2\theta$ function (this is for AM1 results; ab initio calculations show different behavior, which is to be discussed elsewhere[23]). Discussing first the situation for PHBA, the formulated concept is nicely demonstrated in Figure 9 for torsion E, which is not expected to exhibit any steric term; resonance stabilization is maximum when the molecule is planar ($\theta = 0°$ and $\theta = 180°$) and minimum at $\theta = 90°$. Inspection of the torsional angles in Figure 2 (which shows the 180° structure) shows that for torsional angles F and G an additional steric hindrance term is present as is corroborated by Figures 10 and 11. For both angles F and G resonance stabilization is maximum at $\theta = 0°$ and $\theta = 180°$. For angle F there is a steric hindrance term which has a maximum (i.e., most unfavorable situation) at $\theta = 0°$ because the two phenyl rings hinder each other strongly. One would expect the carboxyl oxygen and a phenyl hydrogen to hinder each other at the $\theta = 180°$ configuration (situation depicted in Figure 2), but during full geometry optimization and keeping only the torsional angle fixed, a concerted rotation around torsional angle G was observed. The occurrence of concerted rotations has been plotted in Figures 12–14

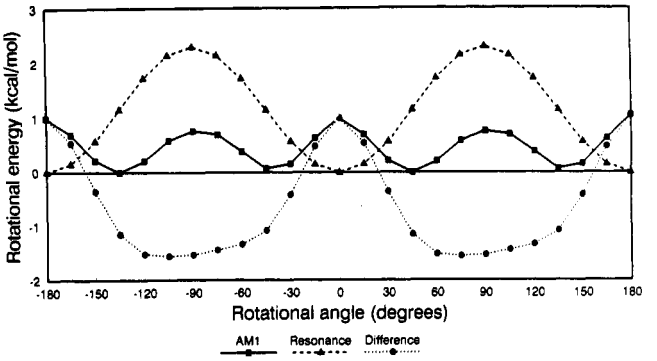

Figure 11. Torsional energy for torsion G of PHBA calculated by the AM1 method, the resonance stabilization energy reflected by a $\sin^2\theta$ dependence, and the remaining energy difference plot. The latter represents the steric interaction energy between a phenyl proton and the carbonyl oxygen. For further discussion see text.

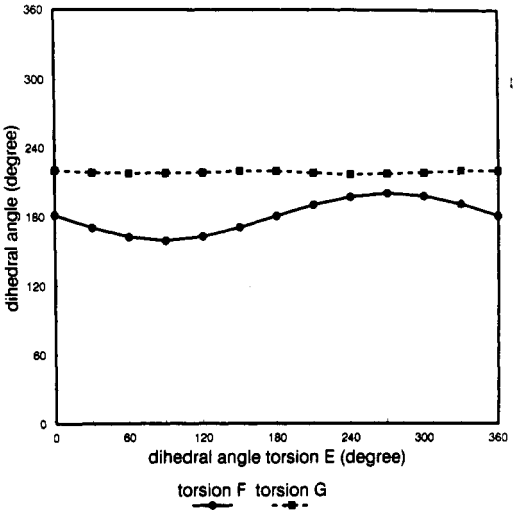

Figure 12. Concerted motion of torsions F and G occurring when torsional angle E is varied in PHBA.

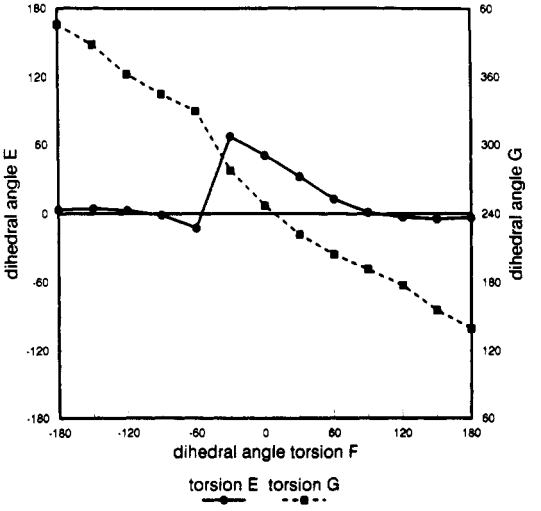

Figure 13. Concerted motion of torsions E and G occurring when torsional angle F is varied in PHBA.

for torsions E, F, and G, respectively. No significant concerted rotation is induced by rotation around the E bond (Figure 12). For the 0° torsional angle of the F torsion one observes a change for both E and G torsional angles by 60° (Figure 13) which minimizes steric hindrance between the phenyl rings. The steric hindrance at $\theta = 180°$ for the G torsion when a phenyl hydrogen and the carbonyl oxygen overlap is not prevented by concerted

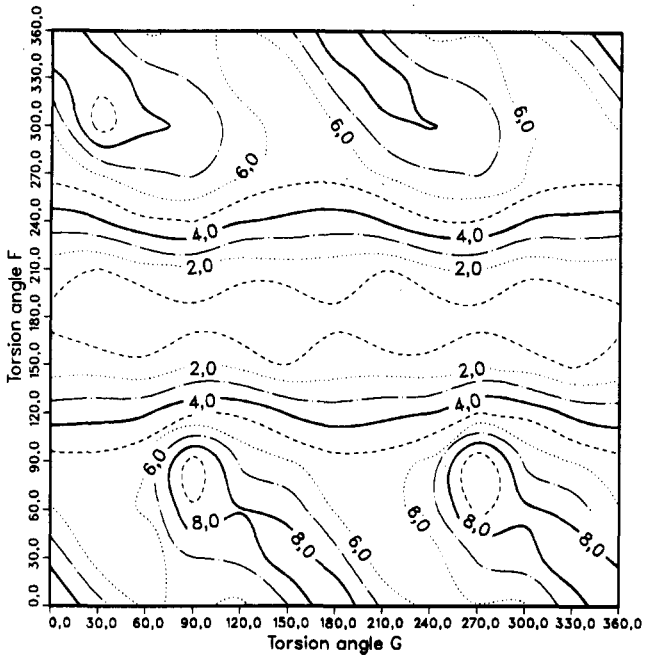

Figure 14. 2-D map displaying the potential energy as a function of rotation around torsional angles F and G in PHBA. The values in the plot are relative energies in kcal/mol. Note that there is an additional variation of the angle E that could not be displayed simultaneously.

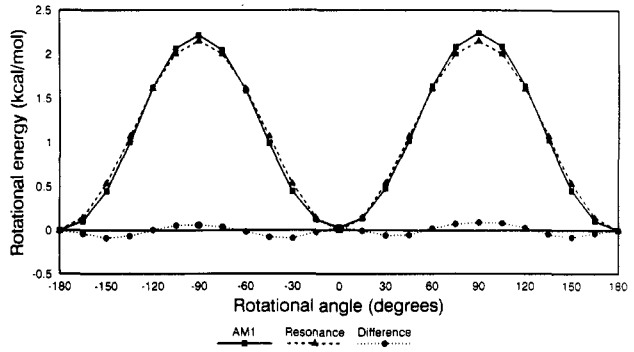

Figure 15. Torsional energy for torsion A of PET calculated by the AM1 method, the resonance stabilization energy reflected by a $\sin^2\theta$ dependence, and the remaining energy difference plot.

motion around torsional angle F (see equator in Figure 14). As a consequence Figure 11 shows steric hindrance maxima both at 0° and at 180°. The maximum resonance stabilization energy depicted in Figure 11 was roughly estimated recognizing the quadratic dependence (in the absence of strong concerted motion) on $\sin\theta$ and the steric hindrance term exhibiting smoothly varying behavior. Returning to Figure 14, we depicted the potential energy surface for rotation around bonds F and G in order to have a more detailed view of concerted behavior. AM1 energy minimizations were carried out by fixing angles G and F with subsequent increase of torsional angle F (inner loop), and after varying angle F from 0 to 360°, angle G was increased (outer loop). From this plot we see that there is quite some concerted motion, in particular where the contours represent high energies.

PET data can be analyzed similarly. Symmetries of steric and resonance stabilization terms again fully agree with a simple explanation obtained when carrying out the rotations in Figure 1. For torsion A (Figure 15) the torsional energy curve is described well by a $\sin^2\theta$ just as for torsion E of PHBA representing resonance interaction only. For torsion B (Figure 16) the resonance stabilization is relatively strong (7 kcal/mol). At $\theta = 0°$ steric hindrance

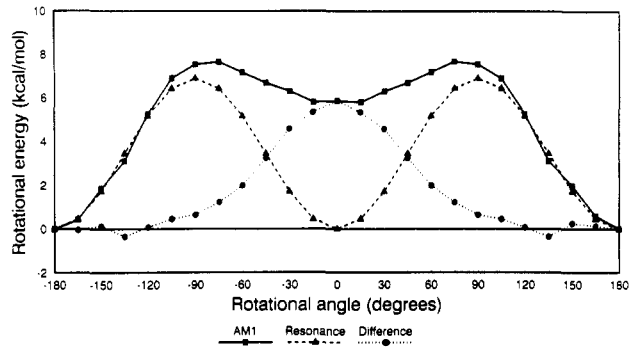

Figure 16. Torsional energy for torsion B of PET calculated by the AM1 method, the resonance stabilization energy reflected by a $\sin^2\theta$ dependence, and the remaining energy difference plot. Steric hindrance is only significant near $\theta = 0$, because of two ethyl hydrogens interacting strongly with the carbonyl oxygen.

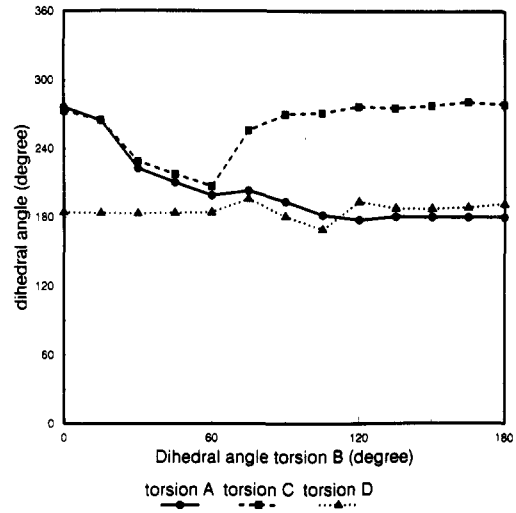

Figure 17. Concerted motion of torsions A, C, and D occurring when torsional angle B is varied in PET.

is at a maximum, with two hydrogen atoms of the ethyl fragment interacting with protons of the phenyl group, and at $\theta = 180°$ it is at a minimum. Torsion C (see Figure 1) evidently shows no resonance stabilization as was to be expected because the ethyl fragment breaks the conjugation, and only a steric hindrance term of approximately the same magnitude as for torsion B shows up.

Torsion D (Figure 1) is the only torsion that definitely shows an asymmetrical rotational energy curve with regard to rotational angle. The curve is carefully checked by starting AM1 optimizations from different initial geometries, but the curve as plotted in Figure 3 was obtained repeatedly. We note however that the structure depicted in Figure 1 lacks a local center of inversion located at the center of the ethyl bond, which must be the reason for this asymmetry.

The concerted motion connected to these rotations has been depicted in Figures 17–19. In particular, a torsion around bond B (Figure 17) causes a strong response of the torsional angles A and C. No figure has been included showing the response of torsions B, C, and D when rotating around bond A, the reason being that virtually no concerted motion was observed in these cases.

Comparing the results obtained for PET and PHBA shows that torsions A and E are essentially the same rotations as corroborated by the calculated energy profiles; the latter can entirely be described by resonance stabilization. The barrier heights for torsions A and E differ by 0.7 kcal/mol though, so why this difference? In order to elucidate this point we calculated the torsional barrier

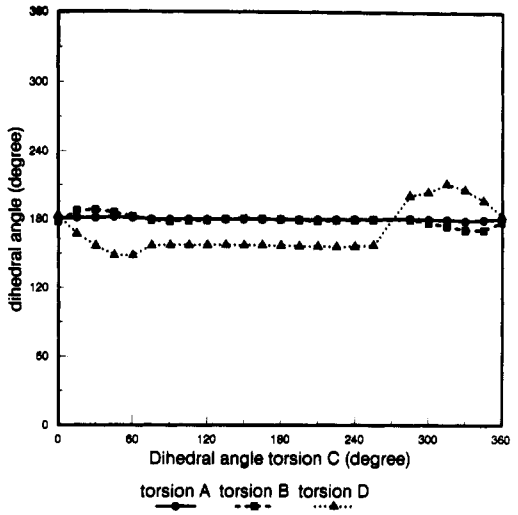

Figure 18. Concerted motion of torsions A, B, and D occurring when torsional angle C is varied in PET.

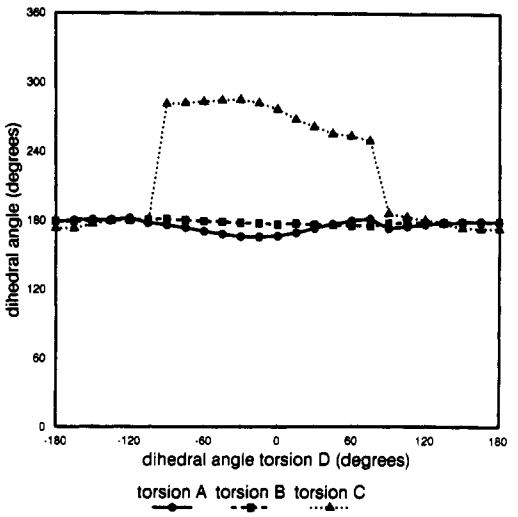

Figure 19. Concerted motion of torsions A, B, and C occurring when torsional angle D is varied in PET.

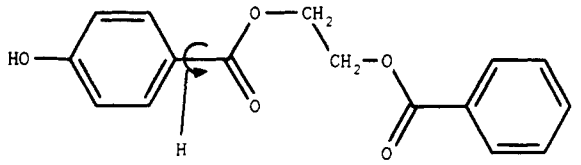

Figure 20. Structure of "modified PET" showing the torsional angle H, studied to investigate the effect of para-substituted end groups on the rotational barrier.

in what we have called "modified PET", i.e., PET in which the methylcarboxyl group has been replaced by an OH group so that it resembles PHBA (see Figure 20). The calculated torsional barrier is compared with that of PET and PHBA in Figure 21. It is concluded that the aforementioned difference in barrier height between torsions A in PET and E in PHBA is entirely due to the (para) substituents on the phenyl ring.

Torsions B (PET) and F (PHBA) also seem rather alike; the expected presence of much stronger overlap between the phenyl rings in PHBA than in PET is prevented by concerted motion as can be deduced from the correlation diagrams Figure 13 (PHBA) and Figure 17 (PET), respectively. Apparently the phenyl rings in PHBA can avoid each other quite effectively and the torsional energy profiles for torsions B (PET) and F (PHBA) are rather similar in both magnitude and form. The other barriers

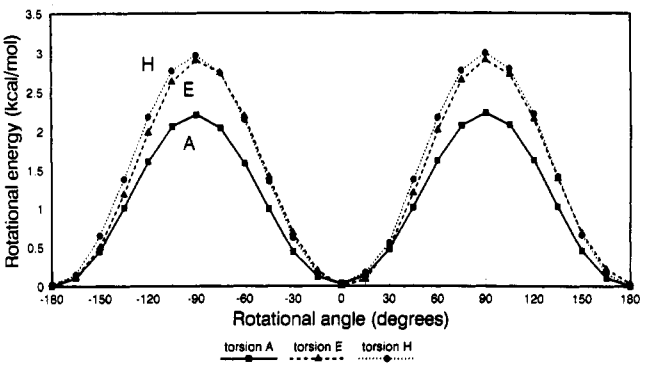

Figure 21. AM1-calculated torsional barriers for the C_{phenyl}–$C_{carbonyl}$ torsions in PHBA (E torsion), PET (A torsion), and "modified PET" (H torsion).

in the two systems cannot be related due to their different geometrical characters.

(b) Force Field Calculations. The results of force field calculations of PET and PHBA involving full geometry optimization using the CVFF (DISCOVER) were depicted in Figures 5 and 6. We will not again discuss the obtained curves for rotational energy versus rotational angle in terms of resonance stabilization and steric hindrance contributions: the similarity in functional form of the CVFF curves and the curves obtained from the AM1 calculations (Figures 3 and 4) points to a similar interpretation.

Quantitatively, however, there are considerable differences between the AM1- and CVFF-calculated results. For PET the CVFF barriers for torsions A and B are 17 kcal/mol, whereas the AM1-calculated barriers are 2.2 and 7.7 kcal/mol, respectively. The CVFF barrier for the C torsion is 9.5 kcal/mol versus 5.5 kcal/mol from AM1. It was not possible to obtain reliable CVFF data concerning torsion D in PET because during energy minimization the molecule tended to fold, placing the phenyl rings in conjunction. We have tried to prevent this by extending the length of the molecule by adding more repeat units but this resulted in back-folding at one of the other ethylene links. Constraining all the torsions in the other links was not considered an alternative as long as the effects on the torsional barrier under consideration had not been thoroughly investigated. Nevertheless we think that, considering the obtained data, it may be stated that the CVFF-calculated barrier for torsion D in PET is 5–6 kcal/mol. We then conclude that the CVFF-calculated torsional barriers in PET are all higher than the equivalent AM1-calculated values, the most striking observation being the A torsion (C_{phenyl}–$C_{carbonyl}$) showing a factor of 7 difference.

Turning to PHBA now, the result found for the E torsion (C_{phenyl}–$C_{carbonyl}$) was similar to that for the A torsion in PET: 17 kcal/mol from CVFF versus 2.9 kcal/mol from AM1. Torsion F is the only torsion showing more or less similar quantitative behavior of both CVFF and AM1 results, the main difference being the more pronounced maximum at zero torsional angle in the CVFF results. The G torsional barrier from CVFF calculations is much higher than that from AM1-calculated data: 4 kcal/mol versus 1 kcal/mol.

Finally, from a comparison of AM1- and CVFF-calculated barriers in PET and PHBA we may conclude that all CVFF barriers, except the F torsional barrier in PHBA, are considerably higher than those computed by the AM1 method. Taking into account the fact that room temperature corresponds to 0.6 kcal/mol, this implies that the flexibility of a polymer chain at realistic processing or application temperatures (i.e., 200–600 K) as calculated

by means of the semiempirical AM1 method will be much higher than the flexibility calculated on the basis of the CVFF.

The CVFF-calculated barriers for the A and E torsions (both C_{phenyl}–$C_{carbonyl}$) of 17 kcal/mol are far too high compared to the range of experimental data and of ab initio calculated data of similar conjugated systems. We can establish this statement more firmly when comparing the CVFF-calculated barrier for benzaldehyde of 18.4 kcal/mol with the experimental value of 5.1 kcal/mol.[16] For phenol, on the other hand, the CVFF-calculated torsional barrier of 3.0 kcal/mol is not far off the experimental value of 3.5 kcal/mol.[16] It has been our experience so far that the CVFF force field does not yield realistic torsional barriers for aromatic systems that have a carbonyl substituent. This conclusion is of particular importance when discussing the relative contributions of intra- (torsional) and interchain interactions on chain stiffness/flexibility in the section dealing with molecular dynamics simulations using the CVFF.

(c) Ab Initio Calculations. In order to check the dependence of the rotational energy profiles on the method of calculation more carefully, ab initio, AM1, and force field calculations were performed on terephthalic acid. The results obtained by the various methods of calculation (Figure 8) differ substantially. All methods show a maximum for $\theta = 90°$ and equal energies for the $\theta = 0°$ and 180° conformations, whereas the ab initio method yields an absolute minimum at $\theta = 180°$; the latter is caused by the dipole–dipole interaction between the carboxylic groups. This is in agreement with experimental data[24] from which it was inferred that the energy difference is less than 1 kcal/mol but nonzero. We have no explanation at present for the difference between the calculated dipole–dipole interaction energy (≤1 kcal/mol as obtained from ab initio calculated dipole moments) and the calculated energy difference between the $\theta = 0°$ and the $\theta = 180°$ conformations for both the STO-3G and the 3-21G basis sets (about 2.5 kcal/mol). This point will be further discussed elsewhere.[23]

The difference between barrier heights calculated using different basis sets has been studied by Marriott et al.[25] They have accumulated evidence that split-valence basis sets overestimate π-electron transfer in electron-withdrawing groups such as CHO, NO_2, and CO_2Me. These authors discussed the performance of STO-3G and 4-31G basis sets with respect to calculated barriers of rotation and dipole moments.[26] Unfortunately, neither of the two basis sets yields better agreement with experimental data for all cases studied, but it nevertheless seems that their arguments require further investigation, which will be reported elsewhere.[23] These arguments of Marriott et al. would make the STO-3G result more reliable than the split-valence basis set with respect to terephthalic acid, thus yielding good agreement with the AM1-calculated barrier. However, this disagrees with the general statement by Fabian[17] that AM1-calculated barriers are far too low for conjugated systems. We note here that Fabian has only very few data that serve to compare AM1-calculated data with experimental data. Moreover, he has neglected differences between experimental gas-phase and condensed-phase barriers of rotation.[8]

(d) Molecular Dynamics (MD) Simulations. MD simulations were carried out on a series of chains varying from flexible ones (PE) to chains of intermediate stiffness (PET and PHBA) to stiff chains such as polyphenyl (pPh). The results depicted in Figures 22–25 clearly show that the MD results obtained using the CVFF qualitatively reflect the expected relative flexibility of the polymer chains.

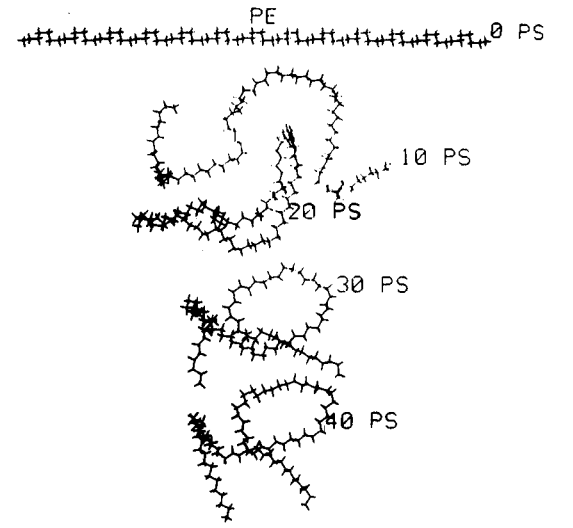

Figure 22. Snapshots from molecular dynamics simulation on polyethylene (PE) employing the CVFF at 10-ps time intervals.

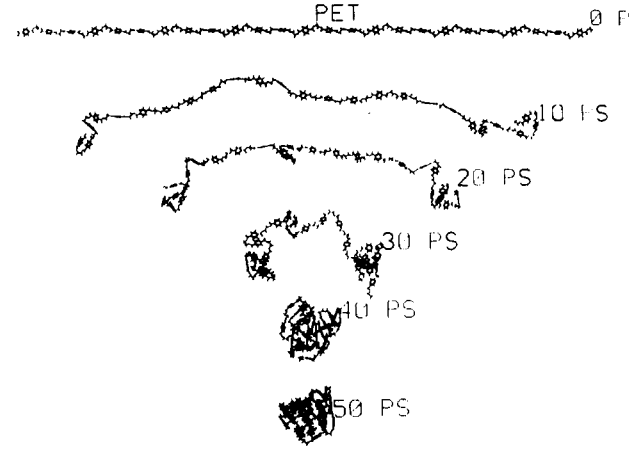

Figure 23. Snapshots from molecular dynamics simulation on poly(ethylene terephthalate) (PET) employing the CVFF at 10-ps time intervals.

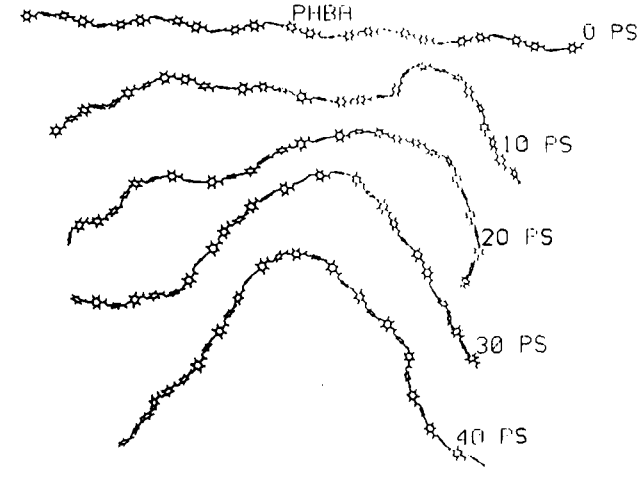

Figure 24. Snapshots from molecular dynamics simulation on poly(*p*-hydroxybenzoic acid) (PHBA) employing the CVFF at 10-ps time intervals.

In the calculation of persistence lengths obtaining reliable numerical data can be difficult because of the influence of the quality of the force field, the type of explicit expression used for calculation of the persistence length,[15] single chain versus bulk simulation, and the extent of the

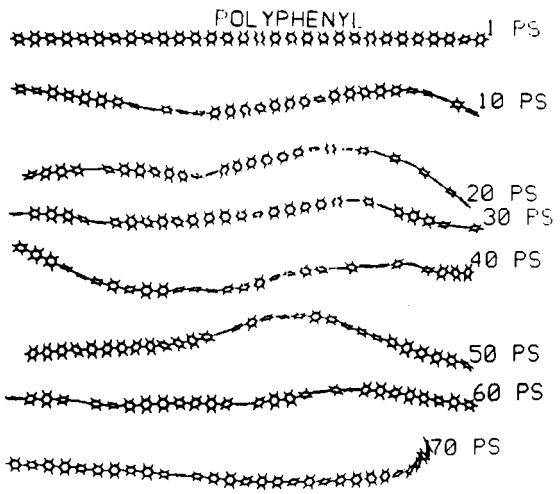

Figure 25. Snapshots from molecular dynamics simulation on polyphenyl (pPh) employing the CVFF at 10-ps time intervals.

MD simulation required in order to obtain good ensemble averages. For an explicit illustration of some of these features, we now turn to the results of our MD simulation on PHBA and compare these with the MD results on PHBA reported by Jung and Schurmann, who employed the AMBER force field and also used a chain of 30 monomer units.[15] From our results the rms deviation from the mean C_{phenyl}–$C_{carbonyl}$–O_{ether} and $C_{carbonyl}$–O_{ether}–C_{phenyl} bond angles were calculated from 6-ps-interval conformations to be approximately 5°. Jung and Schurmann[15] reported values of 4° and 10°, respectively. For the F torsional angle we calculated a rms deviation of 19° (mean 180°, i.e., trans conformation), whereas Jung and Schurmann gave a rms value of 22°. The fact that the rms values given by Jung and Schurmann are close to ours indicates that the aforementioned torsional potentials are almost the same in the CVFF and the AMBER force field.

Jung and Schurmann used several methods for explicit calculation of the persistence length of the PHBA chain and noted that the result of 44 Å obtained by considering the end-to-end distance by applying the expression[15,27]

$$\langle r^2 \rangle = 2a(L - a + a \exp(-L/a)) \qquad (1)$$

(a = persistence length, L = contour length) is far too small. However, applying eq 1 to our MD results ($\langle r^2 \rangle$ and L values), we obtained a value of 94 Å, which according to Jung and Schurmann is in the proper range. So despite the fact that the rms deviations in torsional angles are almost identical, a large difference in calculated persistence length using eq 1 is found, which illustrates the problems encountered when trying to calculate the persistence length. From the present preliminary simulations we cannot give a single and conclusive explanation for this discrepancy, although one of the most important factors certainly is the short simulation time in both our and Jung and Schurmann's simulation. In order to obtain a proper ensemble average for $\langle r^2 \rangle$ one should take a set of starting configurations and analyze after the end-to-end distance has converged to a constant value. Finally, our results show that one cannot disqualify the use of eq 1 on the basis of a single short time span MD simulation, as Jung and Schurmann have done.

From the present MD results we can abstract another important conclusion. In previous sections we argued that the CVFF-calculated barrier heights are too high. A first conclusion seems that a persistence length calculated from the MD results would be too high. However, even chains that are linear in the solid state or in the melt (take liquid crystalline polymers as an example) seem very flexible from the dynamics simulations (Figures 22–25). This leads to the inevitable conclusion that to calculate the chain stiffness and appropriate values for the persistence length as it manifests itself in, for example LCP's, one has to model bulk material, i.e., *include interchain interaction.*

Conclusions

We used force field, semiempirical, and ab initio methods to model rotational barriers in carboxylate-containing aromatic moieties. In separate studies involving the semiempirical AM1 method and the consistent valence force field, it was demonstrated that strong concerted motion between several rotations exists, the correlation being particularly strong for the AM1 results. The presently calculated energy profiles in PET and PHBA can be readily interpreted on the basis of a resonance stabilization contribution and a steric hindrance term contributing to the rotational energy profile.

Concerning absolute barrier heights, we observed relatively large differences between force field, semiempirical, and ab initio results. Unfortunately, no experimental gas-phase data are available for the systems studied in the present work, which makes it impossible to decide which method of calculation is the best. We note that a factor of 2 difference in barrier height, in particular when the heights are comparable to kT, which they usually are, yields quite different results for several calculated properties such as the persistence length when it is calculated from an ensemble average of the fragment configurations. Though not explicitly reported here, similar problems are encountered in calculating the rotational barrier in styrene. These facts indicate that there are problems with modeling rotational barriers in aromatic moieties that have conjugated substituents. Further studies are required in order to find a reliable way of calculating these barriers. We may already note that a comparison of the experimental gas-phase barrier for benzaldehyde with the force field (CVFF) result shows that the force field results obtained are definitely too large.[23]

Using the relatively high barriers from the force field, molecular dynamics simulations showed relatively flexible molecules even for polyphenyl and poly(hydroxybenzoic acid). The results obtained so far suggest that longer simulation times (>50 ps) would show all systems studied to be rather flexible even at ambient temperature and despite the fact that the CVFF barriers to rotation are relatively high. These results indicate that for modeling bulk materials properties it is ultimately necessary to consider "bulk" material or bundles of chains instead of single chains in a vacuum. Further work on Monte Carlo and molecular dynamics simulations is in progress.

Acknowledgment. We gratefully acknowledge Dr. B. Coussens (KU Leuven) for useful comments and for critically reading the manuscript.

References and Notes

(1) Wiberg, K. B.; Murcko, M. A. *J. Am. Chem. Soc.* **1989**, *111*, 4821.
(2) Wiberg, K. B.; Martin, E. *J. Am. Chem. Soc.* **1985**, *107*, 5035.
(3) Schaefer, T.; Penner, G. H. *Can. J. Chem.* **1987**, *65*, 2175.
(4) Coulter, P.; Windle, A. H. *Macromolecules* **1989**, *22*, 1129.
(5) (a) Pedersen, T.; Larsen, N. W.; Nygaard, L. *J. Mol. Struct.* **1969**, *4*, 59. (b) Larsen, N. W.; Nicolaisen, F. M. *J. Mol. Struct.* **1974**, *22*, 29.
(6) Kakar, R. F.; Rinehart, E. A.; Quade, C. R.; Kojima, T. *J. Chem. Phys.* **1970**, *52*, 3803.
(7) Kakar, R. K. *J. Chem. Phys.* **1972**, *56*, 1189.
(8) (a) Fateley, W. G.; Harris, R. K.; Miller, F. A.; Witkowski, R. E. *Spectrochim. Acta* **1965**, *21*, 231. (b) Miller, F. A.; Fateley, W. G.; Witkowski, R. E. *Spectrochim. Acta, Part A* **1967**, *23*, 891.

(9) (a) Konschin, H. Thesis, University of Helsinki, 1985. (b) Konschin, H. *J. Mol. Struct.* **1981**, *77*, 51. (c) Konschin, H. *J. Mol. Struct.* **1983**, *104*, 37. (d) Konschin, H. *J. Mol. Struct.* **1983**, *92*, 173. (e) Konschin, H. *J. Mol. Struct.* **1983**, *105*, 213. (f) Konschin, H. *J. Mol. Struct.* **1983**, *105*, 225.
(10) (a) Heijboer, J. Thesis, University of Leiden, 1972. (b) Heijboer, J.; Baas, J. M. A.; van de Graaf, B.; Hoefnagel, M. A. *Polymer* **1987**, *28*, 509.
(11) Heijboer, J. *Molecular Basis of Transitions and Relaxations*; Meier, D. J., Ed.; Gordon & Breach: London, 1978.
(12) Hehre, W. J.; Radom, L.; Pople, J. A. *J. Am. Chem. Soc.* **1972**, *94*, 1496.
(13) Hummel, J. P.; Flory, P. J. *Macromolecules* **1980**, *13*, 479.
(14) Erman, B.; Flory, P. J.; Hummel, J. P. *Macromolecules* **1980**, *13*, 484.
(15) Jung, B.; Schurmann, B. L. *Macromolecules* **1989**, *22*, 477.
(16) Schaefer, T.; Wildman, T. A.; Sebastian, R. *J. Mol. Struct.: Theochem.* **1982**, *89*, 93.
(17) Fabian, W. M. F. *J. Comput. Chem.* **1988**, *9*, 369.
(18) Vilkov, L. V.; Mastryukov, V. S.; Sadova, N. I. *Determination of the Geometrical Structure of Free Molecules*; Mir Publishers: Moscow, 1983.
(19) Whitley, A.; Yarwood, J.; Gardiner, D. J.; Dave-Edwards, M. P. Paper presented at the Joint Discussion Meeting "Transport Processes in Fluids and Mobile Phases", Aachen, September 1989.
(20) Austin Model 1 has been described in: Dewar, M. J. S.; Zoebisch, E. G.; Healy, E. F.; Stewart, J. J. P. *J. Am. Chem. Soc.* **1985**, *107*, 3902.
(21) Amos, R. D. *The Cambridge Analytical Derivatives Package (CADPAC)*, CCP1/84/4, Computational Science Group, Science and Engineering Research Council, Daresbury Laboratory, Daresbury, Warrington, WA4 4AD, U.K.
(22) INSIGHT/DISCOVER is a molecular modeling software package of BioSym Inc., San Diego.
(23) Coussens, B.; Meier, R. J. To be submitted to *Macromolecules*.
(24) Saiz, E.; Hummel, J. P.; Flory, P. J.; Plavsic, M. *J. Phys. Chem.* **1981**, *85*, 3211.
(25) Marriott, S.; Silvestro, A.; Topsom, R. D. *J. Chem. Soc., Perkin. Trans 2* **1988**, 457.
(26) Marriott, S.; Silvestro, A.; Topsom, R. D.; Bock, C. W. *J. Mol. Struct.* **1987**, *151*, 15.
(27) Kratky, O.; Porod, G. *Recl. Trav. Chim. Pays-Bas* **1949**, *68*, 1106.

Registry No. PET, 25038-59-9; PHBA (homopolymer), 30729-36-3; PHBA (SRU), 26099-71-8; terephthalic acid, 100-21-0.